Available online at www.sciencedirect.com
ScienceDirect
Procedia Engineering 2 (2010) 397–406
Procedia Engineering
www.elsevier.com/locate/procedia

Fatigue 2010

Plain fatigue resistance of shot peened high strength aluminium alloys: effect of loading ratio

M. Benedetti*, V. Fontanari, B. D. Monelli

Department of Materials Engineering and Industrial Technologies, University of Trento, via Mesiano 77, 38123 Trento, Italy

Received 16 February 2010; revised 9 March 2010; accepted 15 March 2010

Abstract

The effect of different shot-peening treatments on the reverse and pulsating bending fatigue behaviour of Al 7075 T651 was studied. The fatigue improvements with respect to the unpeened condition and the influence of the peening intensity on fatigue were discussed accounting for the effects of surface modifications and residual stresses. In particular, the extent of the residual stress redistribution during loading was investigated by means of X-ray diffraction (XRD) measurements. No significant residual stress relaxation was observed in samples tested to a load level corresponding to the fatigue endurance at $5{\cdot}10^6$ cycles. Residual stress relaxation was observed only when the material plastic flow stress was achieved during the compressive part of the fatigue load cycle. Accordingly, shot peened samples with deep sub-superficial compressive residual stress peak showed a reversed fatigue endurance level corresponding to the condition of incipient plastic flow. This phenomenon was also accompanied by sub-superficial fatigue crack initiation. On the contrary, samples tested at shorter fatigue lives or under pulsating loading conditions showed crack initiation close to the surface. The initial and the stabilised residual stress profiles were considered for discussing the improvement in the fatigue behaviour due to peening. For this purpose, a multiaxial fatigue criterion was adopted to account for the biaxial residual stress field. The fatigue life was quite accurately predicted as long as fatigue initiation occurs on the surface.

Keywords: Aluminium alloys; shot peening; fatigue strength; residual stress relaxation; load ratio

1. Introduction

Aluminium alloys look very attractive to the aircraft and automotive industry, steadily seeking an improvement of the energy efficiency of the transport vehicles, because of their high specific static strength. Usually, high static mechanical properties are induced in aluminium alloys by dispersion hardening through solution and ageing heat treatments. However, in contrast with more common metallic materials like steels, they exhibit relatively poor fatigue properties: the fatigue endurance in the high cycle fatigue regime (>5 millions cycle) is about ¼ of the tensile strength [1]. For this reason, aluminium alloys are frequently subjected to surface treatments. For instance, shot peening has always received particular attention, allowing for noticeable increments in the plain fatigue life of steels and light alloys [2,3]. In the literature, the major part of this improvement has been almost unanimously attributed to

* Corresponding author. Tel.: +39-0461-282457; fax: +39-0461-281977.
E-mail address: matteo.benedetti@ing.unitn.it.

1877-7058
doi:10.1016/j.proeng.2010.03.044

the introduction of compressive residual stresses in the surface region, responsible for both retarded fatigue crack initiation and lower small crack growth rates [4].

The authors recently studied the effect of three types of shot peening treatments on the plain fatigue response of the Al-7075-T651 alloy under reverse bending loading conditions (R = -1) [5]. In particular, it was shown that (i) shot peening significantly improves the plain fatigue response of the Al alloy, (ii) the residual stress field does not display an appreciable evolution with the respect to the initial condition at the 5 million cycles fatigue endurance stress, (iii) some relaxation occurs at shorter fatigue lives, the more pronounced the higher the stress level. The plain fatigue response is directly correlated with the surface residual stress as successfully predicted using the Sines criterion incorporating the stabilized residual stress field as mean stresses. However, it was found that the high cycle fatigue behaviour of the more intense peening conditions is rather dictated by the conditions of incipient plastic deformation, as an effect of the superposition between the compressive residual stress with the compressive peak due to the applied reverse bending, in order to preserve the stability of the residual stress field. The numerical investigation conducted in [6] showed that residual stress relaxation observed in [5] is actually due to plastic flow rather than cyclic relaxation.

The present work is aimed at extending these investigations to the case of pulsating bending loading conditions (R = 0). Under these circumstances, the specimen part subjected to tensile bending stresses, where fatigue cracking usually occurs, is prevented from residual stress relaxation caused by compressive plastic deformation. Consequently, under these conditions, the more intense peening conditions are supposed to completely unfold their beneficial effect on the high cycle fatigue strength. Fatigue crack initiation sites have been investigated through scanning electron microscopy (SEM) fractography and the role of surface roughness on the fatigue resistance has been analyzed. Residual stress profiles were used to discuss the improvement in the fatigue response in the hypothesis of crack initiation and early crack propagation as fatigue controlling parameters. For this purpose, a multiaxial fatigue criterion was adopted to account for the residual stress field.

Nomenclature

D_p	mean spacing of adjacent roughness peaks
K_t	stress concentration factor
N	number of cycles
R	stress ratio
R_a	average roughness
R_q	root mean square roughness
R_t	mean value of the peak-valley distance determined on a specific measurement length
$T\sigma$	scatter of fatigue results
σ_{P50} (resp. $_{10\ 90}$)	fatigue endurance with a failure probability of 50% (resp. 10% and 90%)
σ_{0P50}, k	parameters of the S-N curve
$\sigma_{5\cdot10^6}$	fatigue endurance corresponding to $5\cdot10^6$ cycles
σ_a	stress amplitude

2. Materials and experimental procedures

The experimentation has been performed on the aluminium 7075-T651 alloy, widely used for aeronautical applications, supplied in the form of 4 mm thick rolled plate. The bulk material properties have been determined on

five standard monotonic tensile tests (initial strain rate of $1 \cdot 10^{-3}$ s^{-1}) performed in the longitudinal orientation. The results, summarized in Table 1, show a yield strength higher than 500 MPa, combined with a good material ductility (total elongation of 18%).

Table 1. Monotonic tensile properties of the Al-7075-T651 alloy.

E (GPa)	$\sigma_{Y0.2}$ (MPa)	UTS (MPa)	σ_F (MPa)	T.E. (%)	R.A. (%)
73 (±1)	515 (±5)	565 (±5)	760 (±10)	18 (±2)	24 (±2)

E: elastic modulus; $\sigma_{Y0.2}$: 0.2% yield stress; UTS: ultimate tensile strength; σ_F: true fracture stress; T.E.: total elongation; R.A.: reduction in area

The fatigue characterisation has been carried out on prismatic specimens whose geometry, according to the standard ISO 3928, is illustrated in Fig. 1. The microstructure has been tested with the stress axis parallel to the L-direction. The fillet radius is large enough to make any notch fatigue effects negligible. Part of the specimens has been subjected to controlled shot peening: the parameters of the three peening treatments considered are summarized in Table 2 (further details can be found in [5]). Each treatment has been performed using ceramic glass beads, which allow for higher fatigue performances as compared with steel shot. The treatment named CE-B120 employs small ceramic beads leading to a gentle and superficial effect, whereas the second one termed CE-Z425 has been conducted with beads of larger size in order to produce a deeper cold worked layer. The third treatment called CE-Comb is a double peening consisting in the CE-Z425 followed by the CE-B120 treatment.

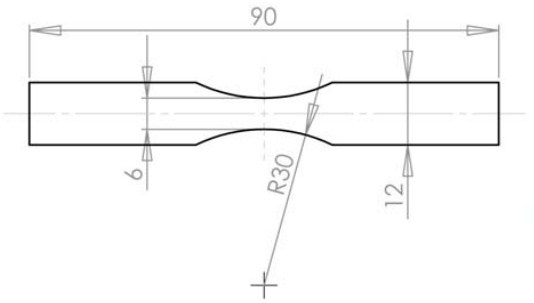

Fig. 1. Plane bending fatigue samples used in this study. Specimen's thickness is 4 mm.

Table 2. Parameters of the three shot peening treatments considered in this study.

Treatment	Bead size (μm)	Bead hardness (HV_1)	Bead composition	Almen intensity	Bead speed (m/s)	Angle of impingement	Coverage (%)
CE-B120	63-125	700	ZrO_2 67%	4.5N	57	90°	100
CE-Z425	425-600		SiO_2 31%	4.5A	26		
CE-Comb	CE-Z425 followed by CE-B120						

Reverse (zero mean stress, R = -1) and pulsating (zero minimum stress, R = 0) plane bending displacement-controlled fatigue tests have been carried out at room temperature air and at a nominal frequency of 30 Hz. Different stress levels corresponding to fatigue lives in the range between nearly $5 \cdot 10^4$ and $5 \cdot 10^6$ cycles have been considered. The fatigue curves corresponding to 50% of failure probability, represented by the S-N curve:

$$\sigma_{P50} = \sigma_{0P50} \times N_f^{-\frac{1}{k}} \tag{1}$$

were determined, following the standard procedure, by fitting the $\log(N_f)$ vs. $\log(\sigma)$ results. The uncertainty range was assumed to be constant and approximated by its centroid value. As a representative value of the scatter, the following expression was used:

$$T\sigma = 1 : \sigma_{P90} / \sigma_{P10} \tag{2}$$

P_{90}, P_{10} denote the 90% and 10% levels of failure probability, respectively. The $5 \cdot 10^6$ cycles fatigue endurance was obtained by a staircase procedure, employing 10-12 samples.

The surface roughness was determined by the centreline average and peak height distributions resulting from a profilometer scan of the specimen surface. The profilometer provides the position of all irregularities having a crest spacing of less than a preset cut-off value.

The analysis of the residual stress field induced by the peening treatments was carried out by measuring the stress profile by XRD technique. They are based on the $\sin^2\psi$ method. The crystallographic direction <422> was chosen with CuKα reflection in order to obtain high angle measurements with higher stress sensitivity. The elastic properties of the alloy were used in the calculation by means of Neerfeld-Hill method [7]. A specific procedure of chemical etching for the progressive thinning of the specimen was employed. The correction accounting for the effect of the removed layer on the residual stress field was performed following the indications reported in [7] and using an appropriate algorithm proposed in [8].

Both initial and stabilized residual stress fields were measured. For this purpose, measurements were performed on specimens tested under reverse bending conditions after failure in a region far enough from the fracture surface (about 2 mm) so that the material rupture was supposed not to have altered the residual stress field. Residual stress profiles measured on run-out specimens were found to be very similar to those determined on failed samples, thus confirming this assumption.

3. Results and discussion

3.1. Surface modifications

The effect on the surface roughness exerted by the shot peening treatments is quantified in Table 3, where the results of profilometer measurements are summarized. The mean value, within an assessment length of 2 mm, of the maximum peak to valley height (R_t) and the mean spacing of adjacent local peaks (D_p) were used to estimate the notch effect exerted by the surface dimples according to the following expression proposed by [9]:

$$K_t = 1 + 4\left(\frac{R_t}{D_p}\right)^{1.3} \tag{3}$$

The values of the estimated K_t for the conditions considered are listed in Table 3. It can be noted that the shot peening treatments introduce a limited-to-moderate stress concentration effect, ranging from 1.08 (CE-B120) to 1.17 (CE-Z425 and CE-Comb).

Table 3. Surface roughness properties.

Condition	R_a (μm)	R_q (μm)	R_t (μm)	D_p (μm)	K_t (Eq. (3))
As-received	0.25	0.30	0.9	-	-
CE-B120	1.35	1.67	6.1	120	1.08
CE-Z425	3.39	4.36	15.2	175	1.17
CE-Comb	3.41	4.37	16.4	190	1.17

Microhardness profiles and the characterization of the cyclic stress-strain response of the shot peened surface layers can be found in [5,6].

XRD measurements were carried out on the fatigue samples in order to characterize the residual stress field prior to fatigue testing. The obtained stress profiles are illustrated in Fig. 2. Notably, the residual stresses introduced by thermo-mechanical treatment as well as by the machining in the as-received condition are one order of magnitude smaller than those measured in the peened samples and will be therefore neglected.

The specimens subjected to the more intense peening treatments (CE-Z425 and CE-Comb) were characterized by deeper compressive residual stress profiles and by higher sub-superficial compressive peaks with respect to the CE-B120 treatment. In this latter case, the surface layer affected by compressive residual stresses is very thin and the peak is located on the surface. The CE-Z425 and the CE-Comb treatments differ slightly in terms of the surface residual stress and sub-superficial peak values, whereas the depth of the compressive peak is nearly the same (0.075-0.080 mm). The difference between the two treatments tends to fade out nearly 200 microns beneath the surface. For all the peening conditions, the peak stress levels reached a considerable value ranging from 0.56 to 0.72 of the material monotonic yield stress.

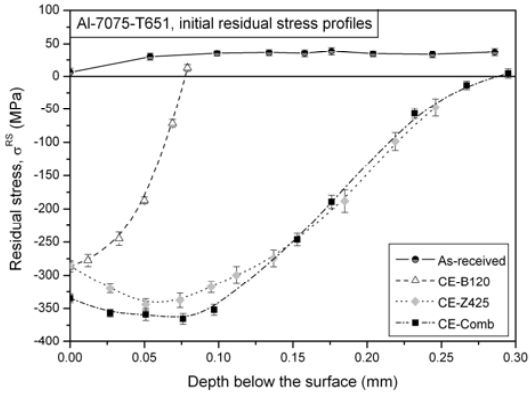

Fig. 2. Initial residual stress profiles of the as-received and peened variants measured by XRD technique.

3.2. Fatigue S-N curves

The results of the reverse (R = -1) and pulsating (R = 0) bending fatigue tests as well as the P_{50} fatigue lines are compared in Figs. 3a and 3b for the different material variants considered, respectively. The parameters representing the fatigue curves corresponding to 50% of failure probability, according to Eq. (1), the results scatter, expressed by Eq. (2), and the fatigue endurance at $5 \cdot 10^6$ cycles are listed in Table 4. All the peening treatments considered were effective in prolonging the fatigue life of the material. This improvement depends on both the applied load and the loading ratio, being more remarkable for load levels corresponding to longer fatigue lives. It can also be observed that the gentlest the CE-B120 treatment induces the highest improvement in the reverse bending endurance limit at $5 \cdot 10^6$ cycles as compared to the more intense peening treatments, i.e. CE-Z425 and CE-Comb (Fig. 3a); on the contrary, the CE-Comb treatment gave the best results for the pulsating bending endurance limit (Fig. 3b). In order to shed light on this apparently anomalous result, an experimental campaign was carried out with the aim of investigating the evolution of the residual stress field during the fatigue life.

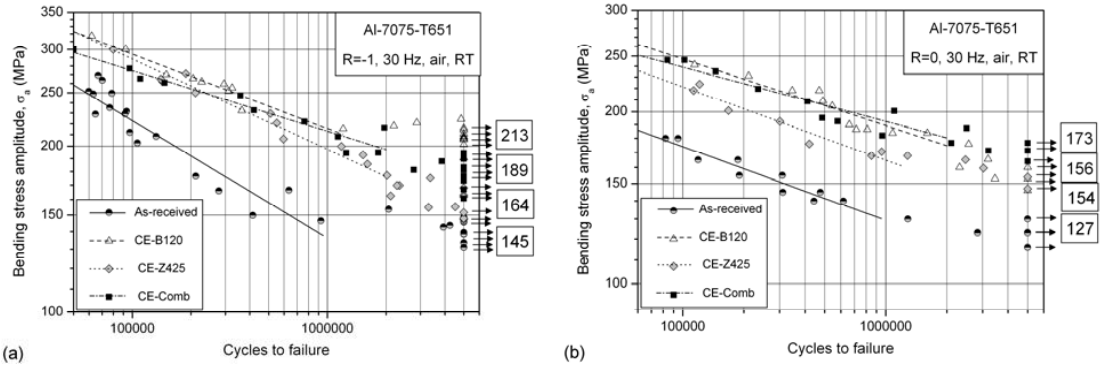

Fig. 3. Reverse (a) and pulsating (b) bending fatigue curves of the as-received and peened conditions. Run-out tests are marked by arrows.

Table 4. Principal results of fatigue tests.

Condition	Endurance limit				Low cycle fatigue					
	$\sigma_{5\cdot10^6}$ (MPa)		St Dev (MPa)		k		σ_{0P5Q} (MPa)		Tσ	
	R = -1	R = 0	R = -1	R = 0	R = -1	R = 0	R = -1	R = 0	R = -1	R = 0
As-received	145	127	8	8	4.68	7.76	2605	770	1:1.20	1:1.15
CE-B120	213	156	4	6	7.38	8.64	1400	935	1:1.11	1:1.15
CE-Z425	164	154	12	8	6.12	7.81	1885	965	1:1.15	1:1.12
CE-Comb	189	173	12	6	9.05	10.60	980	710	1:1.14	1:1.18

3.3. Residual stress evolution during reverse bending fatigue tests

Figures 4a, 4b and 4c illustrate the evolution of the residual stress field in the samples tested under reverse bending conditions at different loading levels for the CE-B120, CE-Z425 and CE-Comb treatment, respectively. It can be noted that some relaxation of the residual stress field occurred at load levels higher than the fatigue endurance, the more pronounced the higher the load levels, whereas the residual stress profiles measured in the specimens tested in correspondence of the fatigue endurance did not show appreciable evolution with respect to the initial residual stress field: the residual stress modification is of the same order of magnitude of the uncertainty band of the XRD measure. This evidence suggests the hypothesis that the relaxation is more like a “quasi-static” effect, due to the achievement of the material’s plastic flow regime [5,6], rather than cyclic relaxation, which should be evident in the high-cycle fatigue regime as well. Accordingly, the fact that the specimens were tested under reverse bending configuration implies the possibility of material’s plasticization when the compressive bending stresses are superimposed to the compressive surface residual stress field.

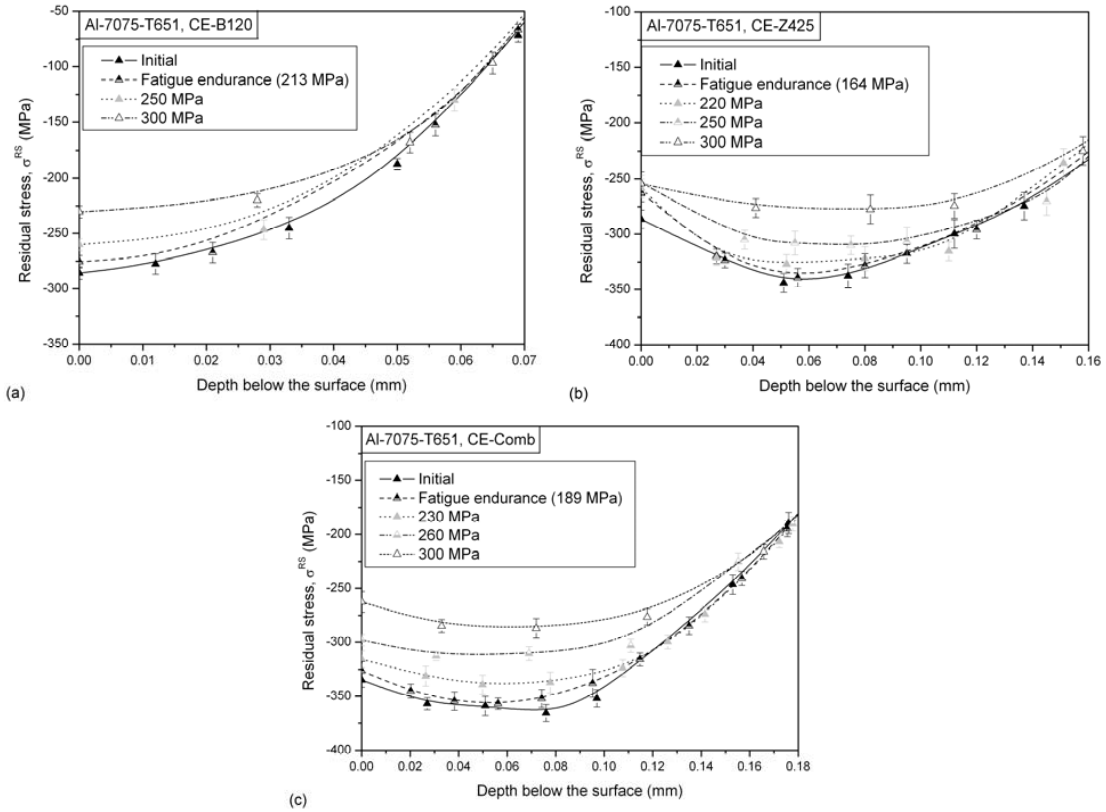

Fig. 4. Comparison between initial and stabilized residual stress profiles measured on the fatigue samples tested under reverse bending conditions and subjected to (a) CE-B120, (b) CE-Z425, (c) CE-Comb shot peening.

This hypothesis has been confirmed by the investigations made in [5,6] based on the cyclic mechanical properties of the shot peened layers. In particular, it has been found that the reverse bending fatigue endurance of the more intense peening conditions is dictated by the condition of incipient plastic deformation during the compressive part of the bending load cycle. On the contrary, in the case of pulsating bending fatigue, the specimen part subjected to tensile bending stresses, where fatigue initiation has been observed, residual stress relaxation due to compressive plastic deformation can not occur, so in the following it will be assumed that the residual stress fields remain stable during pulsating bending fatigue. Obviously, this assumption needs to be experimentally verified in the next by XRD measurements.

3.4. Fracture surfaces analysis

SEM analysis was carried out on the fracture surfaces of the specimens tested at load levels close to the fatigue endurance under reverse (Fig. 5) and pulsating (Fig. 6) bending conditions. In the first case, the observations revealed sub-superficial fatigue crack initiation for the CE-Z425 (Fig. 5b) and CE-Comb (Fig. 5c) treatments, in a region comprised between 200 and 300 μm below the surface, where incipient compressive plastic deformation has been predicted. On the contrary, the crack nucleation was found to occur close to the surface (~20 μm below the surface) in the CE-B120 (Fig. 5a) condition. Furthermore, superficial fatigue crack onset was detected in the samples tested at stress levels leading to failure within $4 \cdot 10^5$ cycles, even in the samples subjected to the CE-Z425 and CE-Comb conditions (here not reported for the sake of brevity).

In the case of pulsating bending fatigue tests, however, fatigue crack initiation has been observed in a region close to the surface (0-100 μm) for all the peened variants considered, as shown in Fig. 6a, 6b and 6c for the CE-B120, CE-Z425 and CE-Comb, respectively. Apparently, due to the absence of compressive plastic deformation, no sub-superficial crack onset occurred.

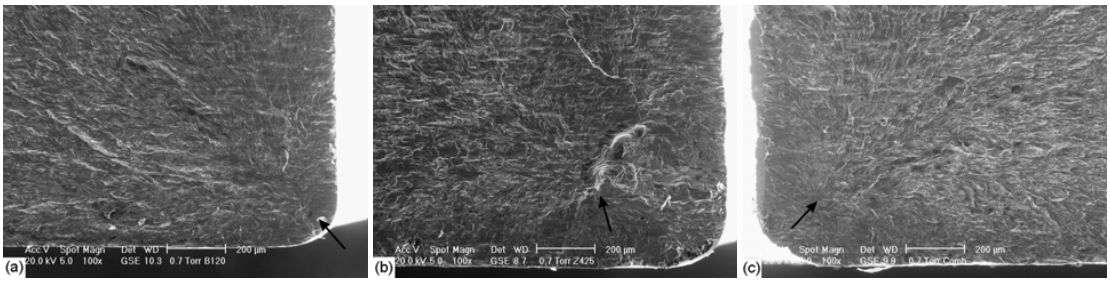

Fig. 5. SEM micrographs of the fracture surfaces around the fatigue crack initiation sites for specimens tested at the fatigue endurance stress under reverse bending conditions. (a) CE-B120 (σ_a = 221 MPa, N = 2.87·10^6 cycles), (b) CE-Z425 (σ_a = 155 MPa, N = 3.30·10^6 cycles), (c) CE-Comb (σ_a = 188 MPa, N = 3.86·10^6 cycles) conditions. Crack initiation sites are marked by arrows.

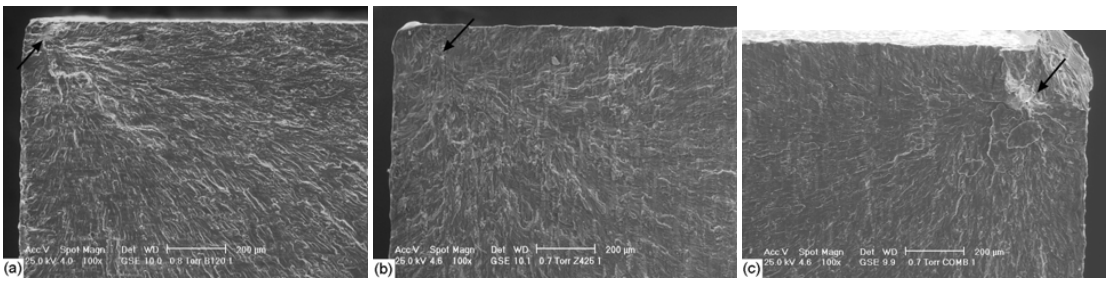

Fig. 6. SEM micrographs of the fracture surfaces around the fatigue crack initiation sites for specimens tested at the fatigue endurance stress under pulsating bending conditions. (a) CE-B120 (σ_a = 165 MPa, N = 3.19·10^6 cycles), (b) CE-Z425 (σ_a = 160 MPa, N = 3.03·10^6 cycles), (c) CE-Comb (σ_a = 187 MPa, N = 2.51·10^6 cycles) conditions. Crack initiation sites are marked by arrows.

4. Simulation of the fatigue response

A numerical model was developed in order to account for both the surface roughness and the residual stresses on the fatigue behaviour. The effect of the surface roughness was taken into account by incorporating into a fatigue criterion the stress concentration factor determined in Section 3.1. Residual stresses were treated as mean stresses superimposed to the oscillating stresses introduced by the external cyclic load [10]. Because of the equibiaxiality of the residual stress field, a multiaxial fatigue criterion was employed. Therefore, the Sines criterion was adopted for modelling the stress conditions as discussed in [5]. Two main assumptions were made: (i) the material's work hardening introduced by the shot peening exerts a negligible influence on the fatigue resistance; therefore, the intrinsic fatigue resistance of the peened material was assumed to be the same as that of the base material. (ii) The fatigue crack initiation occurs on or close to the specimen surface. This was confirmed by experimental investigations, except for the specimens subjected to the two more intense treatments in the high cycle fatigue regime under reverse bending conditions. This fact will be discussed in the following. The initial and the stabilized (only for the samples tested under reverse bending) values of residual stresses on the surface (according to the second assumption) were considered for evaluating the fatigue response in the hypothesis that the initiation life takes a preponderant part of the total fatigue life.

The comparison between the experimental data and the calculated mean fatigue curve is illustrated in Figs. 7a, 7b and 7c for the CE-B120, CE-Z425 and CE-Comb conditions, respectively. It can be noted that, except for the high cycle reverse bending fatigue response of the more intense peened conditions, the fatigue strength is well predicted

by the Sines criterion, particularly when the stabilized residual stresses (SRS) are considered. Conversely, a slight overestimation of the fatigue strength, especially at the higher load levels, is obtained when the initial residual stresses (IRS) are incorporated into the fatigue criterion. Apparently, the beneficial effect of the residual stresses on the fatigue response is partly reduced by the residual stress relaxation. On the contrary, the proposed approach cannot describe the high cycle reverse bending fatigue behaviour of the two intense peening treatments (Figs. 7b and 7c), whose $5 \cdot 10^6$ cycles fatigue endurance was found to correspond to the condition of sub-superficial incipient plasticization (whose stress level is indicated in Figs. 7b and 7c), phenomenon that cannot be captured by the multiaxial fatigue criterion. Noteworthy, the two material conditions subjected to the more intense peening conditions displayed a high cycle fatigue response that is fairly independent of the loading ratio, i.e. the mean stress level.

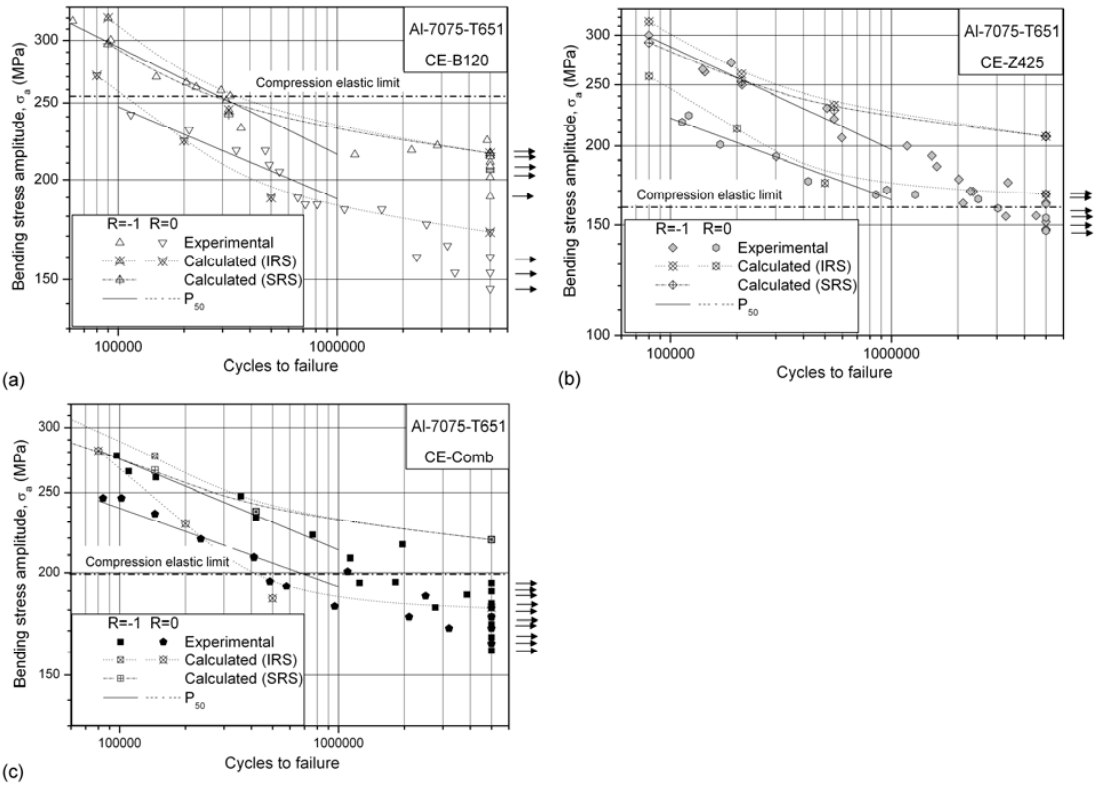

Fig. 7. Comparison between experimental and calculated P_{50} fatigue curves of the peened conditions. (a) CE-B120, (b) CE-Z425, (c) CE-Comb peening treatment. IRS: initial residual stresses, SRS: stabilized residual stresses. The fatigue regimes leading to compression plasticization are indicated as well.

5. Conclusions

The effect of the loading ratio on the bending fatigue resistance of shot peened 7075-T651 aluminium alloy was investigated. Experiments were conducted on specimens subjected to three different shot peening treatments and tested under reverse and pulsating bending fatigue. Surface roughness was measured to characterize the impact of the peening treatment upon the fatigue response. XRD measurements were carried out to determine the initial and the stabilized residual stress field. Conditions for compression plasticization of the material during the reverse bending fatigue life, leading to quasi-static residual stress relaxation, were identified. SEM investigations on the

fracture surfaces were performed to identify fatigue crack initiation sites. An analytical model was built up for predicting the fatigue resistance taking into account the effect of both residual stresses and surface roughness. It has been found that the high cycle fatigue response can be quite accurately predicted for both loading ratios considered, provided that no compressive plastic deformation occurs. These findings can be advantageously used to correctly design, for a specific application, the optimal shot peening treatment also accounting for the load ratio experienced in service by the component.

Acknowledgements

Mr. M. Bandini, Peen Service, Bologna, Italy, is gratefully acknowledged for conducting the shot peening treatments.

References

[1] ASM handbook, Properties and selection: nonferrous alloys and special-purpose materials, Vol. 2, 10th edition, Materials Park, Ohio: American society for metals, 1991.

[2] Wagner L, Lütjering G. Influence of shot peening on the fatigue behaviour of Ti-alloys. In: *Shot Peening*. Oxford: Pergamon Press, 1981, pp. 453-460.

[3] Benedetti M, Fontanari V, Höhn B, Oster P, Tobie T. Influence of shot peening on bending tooth fatigue limit of case hardened gears. *Int. J. Fatigue* 2002;**24**:1127-1136.

[4] Wagner L. Mechanical surface treatments on titanium, aluminum and magnesium alloy. *Materials Science and Engineering* 1999;**A263**:210-216.

[5] Benedetti M, Fontanari V, Scardi P, Ricardo CLA, Bandini M. Reverse bending fatigue of shot peened 7075-T651 aluminium alloy: The role of residual stress relaxation. *Int J Fatigue*. 2009;**31**:1225-1236.

[6] Benedetti M, Fontanari V, Monelli BD. Numerical simulation of residual stress relaxation in shot peened high-strength aluminium alloys under reverse bending fatigue. *ASME J. Engng Mater. Techn.* 2010;**132**:011012-1-9.

[7] Noyan IC, Cohen J.B. Residual stress measurement by diffraction and interpretation. Ed. Springer-Verlag New York 1987.

[8] Residual stress measurement by X-ray diffraction-SAE J784a, SAE Information Report, Second edition, 1971.

[9] Li JK, Yao Mei, Wang Duo, Wang Renzhi. An analysis of stress concentration caused by shot peening and its application in predicting fatigue strength. *Fatigue Fracture Engng Mater. Struct.* 1992;**15(12)**:1271-1279.

[10] Flavenot JF, Skalli N. A comparison of multiaxial fatigue criteria incorporating residual stress effects. In: *Biaxial and multiaxial fatigue*, Eds. M. W. Brown, K. J. Miller Mechanical Engineering Publications London (1989) pp.437-457.